VDMA
Fluid Power Association

22nd ISC

International Sealing Conference

Stuttgart, Germany
October 01 - 02, 2024

Sealing Technology –
Challenges accepted!

IMA
UNI STUTTGART

ISBN 978-3-8163-0768-6

Fachverband Fluidtechnik im VDMA e. V. Lyoner Str. 18
50628 Frankfurt am Main
Germany

Phone +49 69 6603-1513
E-Mail maximilian.baxmann@vdma.org
Internet www.vdma.org/fluid

Simulation of Leakage Flow in dynamic seals from 3D-printing

Matthias Graf, Tobias Lankenau, Kathrin Ottink, Thomas Ebel

Additive Manufacturing (AM) technologies are advancing rapidly, even within the realm of seal production. However, the surface quality of AM seals typically falls short when compared to seals manufactured conventionally. For instance, Fused Filament Fabrication (FFF) yields components with a characteristic string-like surface texture. The dimensions of this texture align with the fluid film thickness of a dynamic rod seal. Through a fluid-structure interaction (FSI) simulation employing coupled Navier-Stokes equations, the fluid flow between the seal and rod can be analyzed. This simulation demonstrates that periodically fragmented contact has a significant impact on the sealing properties of the dynamic seal. A comparison between traditional seals and those produced via FFF manufacturing reveals notable implications, such as alterations in the reverse feed rate through the seal gap.

1 Introduction

Additive Manufacturing has made significant strides in recent years and presents itself as a viable alternative for seal production. Seals, being components subjected to wear due to tribological factors, require periodic replacement. The availability of spare parts can be improved through fast and on-demand additive manufacturing. Fused Filament Fabrication (FFF) emerges as a promising production method, particularly for TPU-based dynamic rod seals [1]. Experimental studies have indicated that careful selection of printing parameters and materials results in seals boasting impressive sealing properties [2]. Although the lifespan of FFF seals may be shorter compared to their conventionally manufactured counterparts, they serve as a quick and interim solution to prevent costly machine downtime.

However, the manufacturing process yields seals with slightly different surface structures than those from conventional methods. In FFF production, a thermoplastic filament is extruded through a heated nozzle and deposited in a viscous state. As the nozzle moves over a build platform, a structure is gradually formed, with the molten filament cooling at ambient temperature. Figure 1 illustrates a cross-section of a seal produced using this method. The notable differences in material distribution, compared to seals from conventional production, include:

1. Porosity between individual printing strands.

2. Surface topography characterized by a series of arcs rather than smoothness.

While the presence of pores (porosity) is not the primary focus of this research, as they are isolated and non-connected, the non-smooth surface topography exhibits a periodic structure at a length scale deemed relevant for sealing properties, particularly in fluid transport during the in- and outstroke. This periodic surface structure operates at a scale of a few hundred micrometers, contrasting with the significant role played by the design of the seal lip geometry, a fundamental aspect of dynamic

seal design [3]. The provided source offers fundamental equations for analytical fluid flow calculations during the in- and outstroke phases.

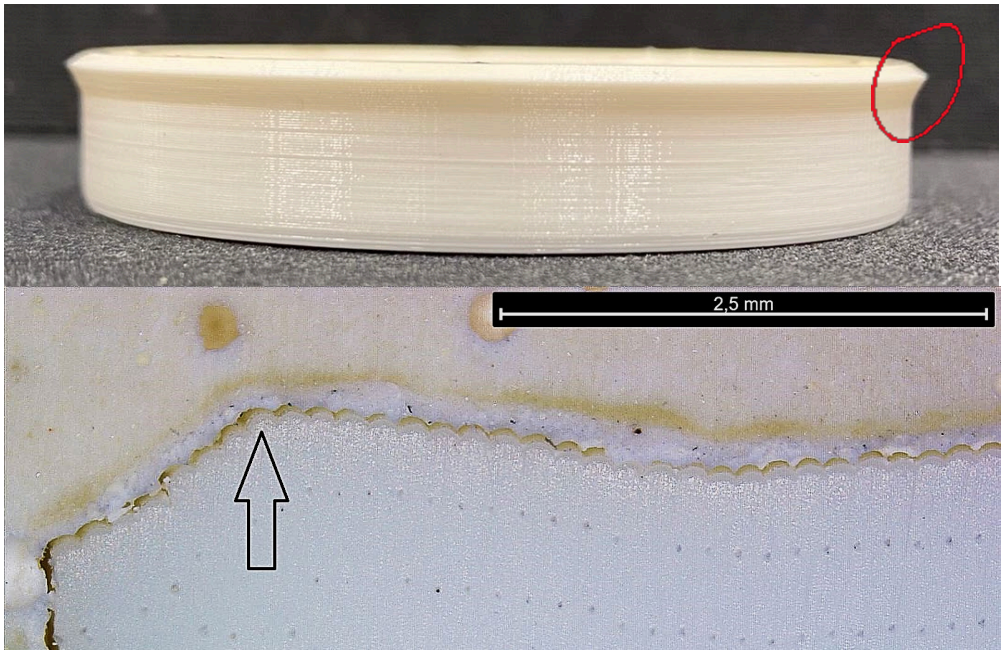

Figure 1: Surface structure and crossection of one dynamic rod seal manufactured by FFF. Arrow marks the seal lip.

A seal is typically considered tight when the reverse fluid flow through the seal is equal to or higher than the leakage flow during the outstroke. Therefore, this study focuses on assessing the capability of seal geometry to facilitate reverse fluid flow during the instroke.

2 Short state of the art

The simulation of fluid motion within a seal gap can only be analytically solved for a limited number of cases. One of the initial solutions was presented by Blok, referred to as the "inverse Theory" [4]. Generally, the flexibility of the seal introduces fluid-structure interaction (FSI). Early numerical solutions with slightly varied approaches were presented by Öngün [5] and Salant [6].

Currently, FSI simulations conducted through commercial software represent the state of the art. These software tools typically resolve the Reynolds equation for thin film flow and leverage the rotational symmetry of the system. Lankenau [7] demonstrated an instance where the Navier-Stokes equations were solved instead of the Reynolds equation for a seal application.

The sources mentioned above primarily focused on situations with microscopically smooth contact. Microscopic roughness of the seal was considered by [8]. However,

the roughness examined in that study does not align with the typical surface structure produced by FFF. The FFF-generated surface structure is notably periodic, characterized by arcs arranged in rows with tip-to-tip distances of a few hundred micrometers. Studies on fluid flow simulations for the instroke motion of 3D printed seals are not yet publicly available.

3 Model definition

3.1 Physical modelling: Geometry, Parameters, Domains, Boundaries

The model system parameters are detailed in Table 1, and the geometry is illustrated in Figure 2. The intersections of geometry between the seal, rod, and groove indicate that the seal is statically energized to ensure sealing functionality.

Table 1: Parameter list for the simulation.

Variable	Name	Numerical value and Unit
v	rod velocity	$0 \dots 2.0\ \frac{m}{s}$
$p_{ambient}$	ambient pressure	$0\ bar$
$p_{cylinder}$	cylinder pressure	$1.5\ bar$
d_{Rod}	rod diameter	$50\ mm$
η_{Oil}	dynamic oil viscosity	$0.2\ Pa \cdot s$
ρ_{Oil}	oil density	$850\ \frac{kg}{m^3}$
Δs	contact offset in seal gap	$2\ \mu m$
C_1	Neo-Hooke stiffness parameter for seal	$8\ MPa$

Two geometry cases are currently under investigation: the "reference" geometry, which represents the seal from conventional manufacturing without microscopic surface structure, and the "FFF" geometry, which is identical to the reference geometry except for the presence of surface structure at the seal lip (Figure 2). In the FFF geometry, the surface is depicted by a series of arcs. It was ensured that the outermost tip point of both geometries was identical to maintain the same macroscopic pretension in contact with the rod and groove.

The cylinder fluid pressure was set to $1.5\ bar$, and the rod was operated from standstill to a sliding velocity of $2\ m/s$ for the instroke (upward motion in Figure 2). The entire free space around the seal was filled with hydraulic oil. During instroke motion, this represents the scenario that demonstrates the maximum inward fluid transportation capability of the system. In practical terms, only the amount of fluid available on the rod surface can be transported into the cylinder.

The fluid is modeled using the Navier-Stokes equations without compressibility. Laminar flow behavior is ensured due to small Reynolds numbers. Cavitation effects are not anticipated to be dominant and are therefore neglected. The in- and outflow of the cavity where pressure is applied are subjected to Dirichlet boundary conditions. The solid seal, modeled as hyperelastic and incompressible, follows a Neo-Hook material model. Solid friction is not taken into account in the model.

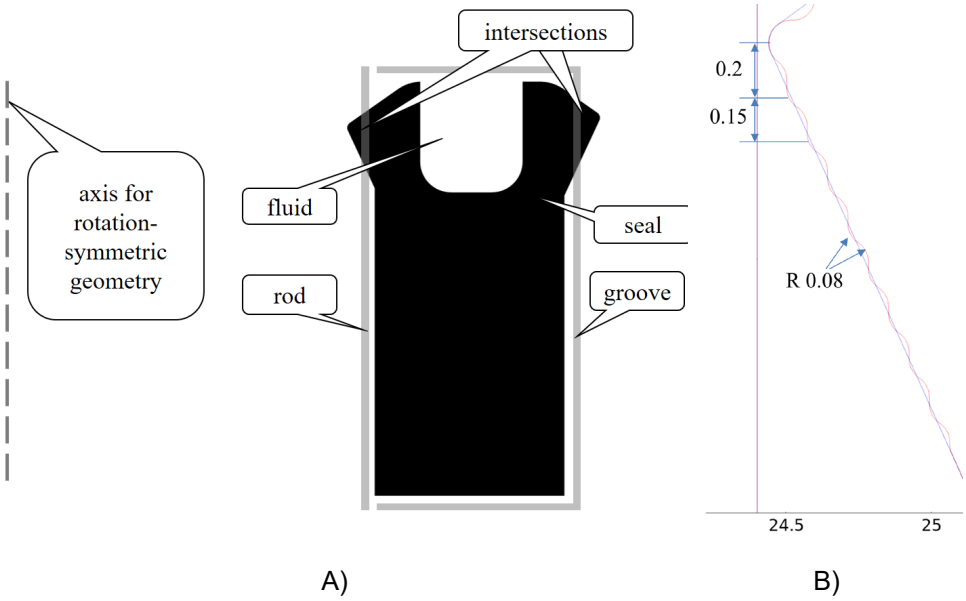

Figure 2: A) Geometry of the simulated seal in unloaded case. Position of the axis for rotation symmetry only for indication, not to scale. Upper side is cylinder side. Lower side is ambient side. B) Blue: Smooth reference surface geometry. Red: FFF surface geometry. Length in Millimetres.

The free interface between the fluid and solid is described by fully coupling the balance of forces, mass conservation, and continuity. No-slip conditions are applied to all rigid interfaces (groove, rod) or solid interfaces (seal).

3.2 Numerical solution: Solver, Elements, Steps, Contacts

The coupled FSI problem is formulated using Arbitrary Lagrangian Eulerian (ALE) coordinates. For practical modeling and numerical solution, the software tool "COMSOL Multiphysics" is utilized. The solvers employed are "MUMPS" and "PARDISO," which compute a quasistatic solution. The simulation is conducted in two steps.

- Initially, for the pretensioned seal, the fluid is not included. A "too-small" rod and a "too-big" groove are initially modeled. With the assistance of rigid body motion, the geometry is corrected, and the seal is pretensioned (see Figure 3A). The contact between the seal and rod is incorporated using a Lagrange contact condition with a permanent offset $\Delta s = 2\ \mu m$. This method, proposed

by v. Wahl [9], ensures that a minimum fluid gap between the seal and rod is always maintained. The seal is modeled using linear triangle elements, with element side lengths ranging between $0.00268\ mm$ and $0.188\ mm$.

- Following the pretension buildup, the fluid is included in the simulation. The triangular fluid elements operate using quadratic shape functions, with element side lengths defined up to $0.5\ \mu m$. These elements are inserted into the gap with a smallest discretization of 13 elements for the seal gap height (see Figure 3B). In the simulation, the velocity of the rod is increased from standstill to $2\ m/s$.

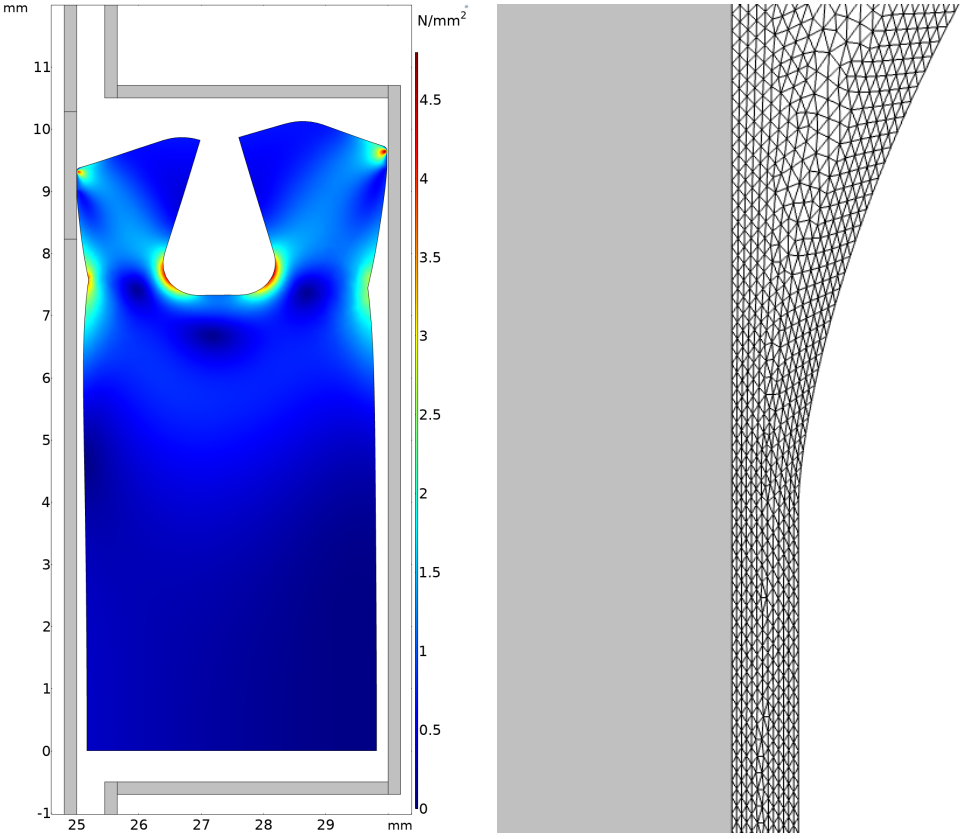

Figure 3: A) Configuration of pretensioned seal in contact with grove and rod. Color code: Von Mises equivalent stress. B) Element size for the fluid mesh in the seal gap.

The entire simulation time on a conventional workstation lasted approximately 3 hours. The analysis of results focused on fluid pressure and surface load on the seal.

4 Simulation Results and Discussion

4.1 Smooth reference geometry

Initially, the simulation focuses on the smooth reference surface geometry. Upon applying the fluid pressure in the cylinder ($1.5\ bar$), the rod undergoes acceleration for upward instroke motion. Consequently, it tends to transport hydraulic fluid from the ambient low-pressure side into the pressurized cylinder, resulting in an acting pressure difference in the cylinder. Figure 4 illustrates the increase of the elastohydrodynamic pressure peak in the converging gap. With increasing sliding velocity, the pressure peak opens the seal gap.

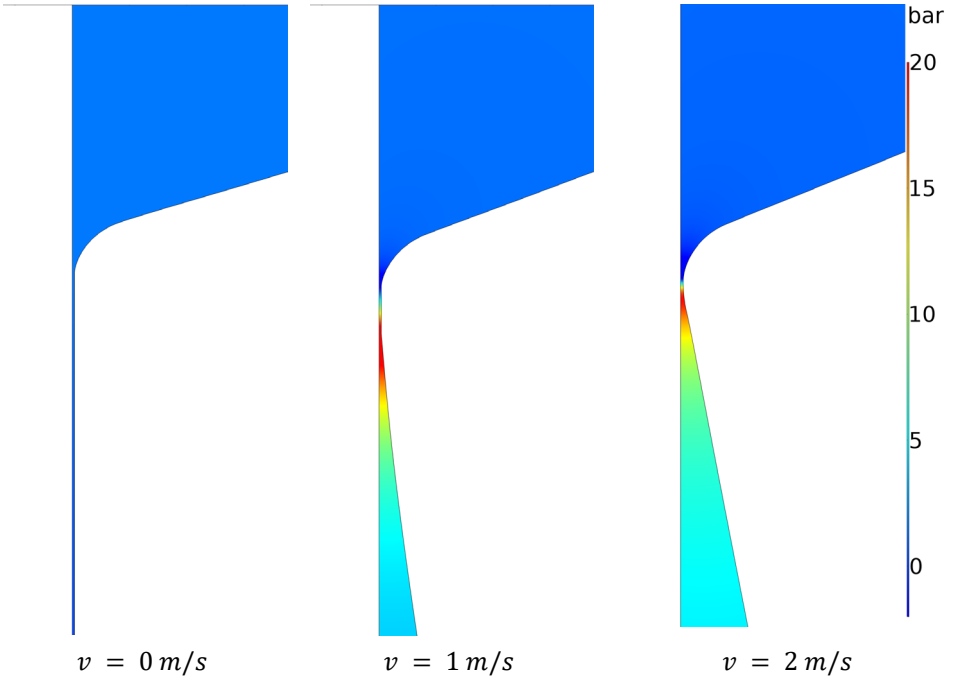

Figure 4: Fluid pressure distribution in the seal gap at different rod velocities for the smooth reference seal.

The seal lip experiences loading from two pressures: one resulting from the solid body contact with the rod and the other from the hydrodynamic fluid. Both are depicted in Figure 5. At lower sliding velocities, the solid body pressure predominates, while at higher velocities, the hydrodynamic pressure becomes dominant. It's evident that the fluid pressure acts on a significantly larger contact area compared to the contact force, resulting in a less pronounced local stress peak in the seal material. To obtain the total force on the seal lip, the stress has been surface integrated. Figure 6 illustrates how increasing rod velocity continuously converts contact force into fluid force.

For sliding velocities lower than approximately $1.86\ m/s$, a residual solid body contact is retained, with the minimum distance between the rod and seal at $\Delta s = 2\ \mu m$. However, at a sliding velocity of $1.86\ m/s$, solid body contact is lost, and only fluid forces remain. At this velocity, the minimum distance between the seal and rod increases to $2.6\ \mu m$.

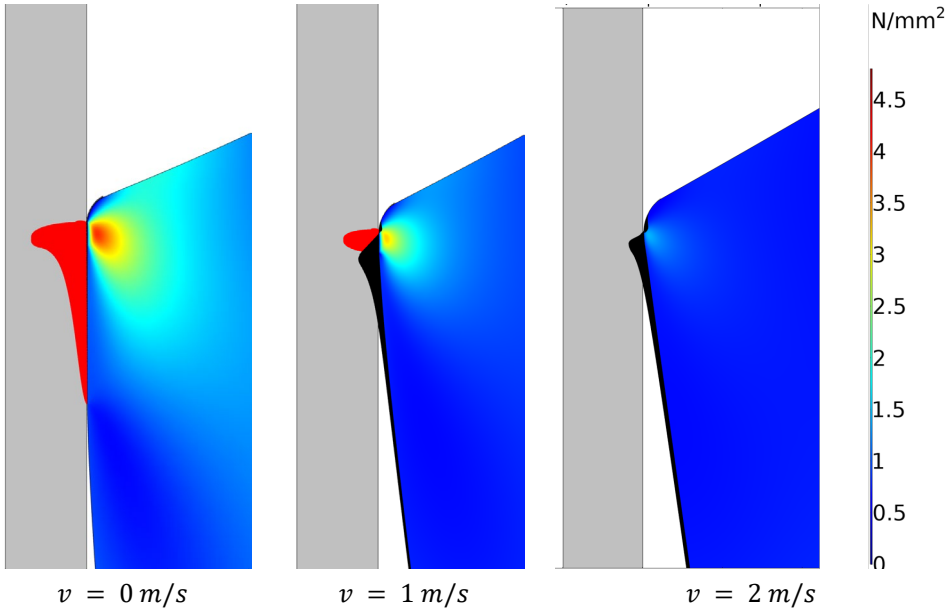

Figure 5: Contact pressure on the seal with smooth reference geometry. Red: Load from solid body contact between seal and rod. Black: Hydrodynamic load from the fluid.

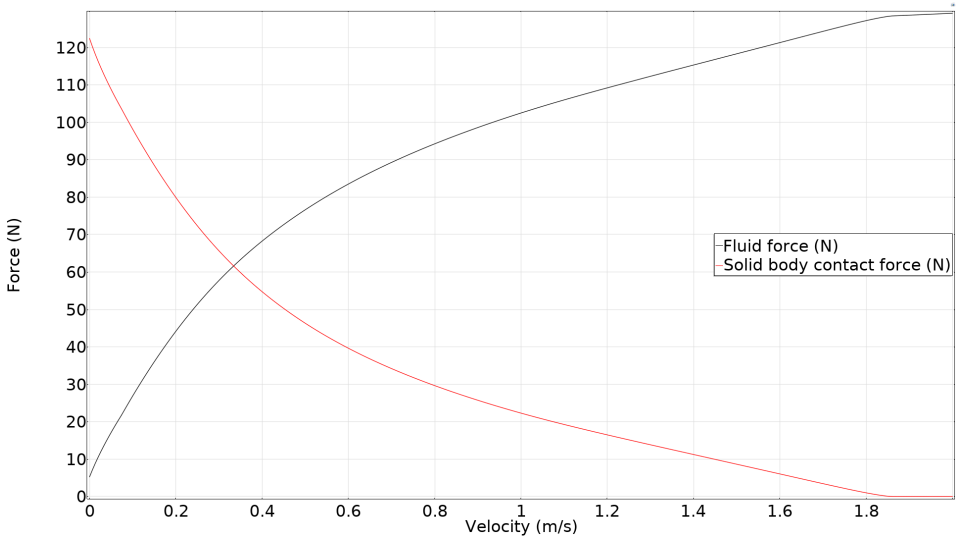

Figure 6: Velocity dependency of the load for the smooth reference geometry.

4.2 Fused Filament Fabrication (FFF) geometry

The same simulation was conducted again, this time utilizing the FFF surface geometry. Upon pressing in, three of the seal lip surface strings make contact with the rod surface. Consequently, FFF manufacturing results in a surface contact that is fragmented into several contact regions. These individual contact regions exhibit a locally nearly Hertz-like pressure distribution, as depicted in Figure 7. As the sliding velocity increases, the fluid pressure peak develops in front of the first contact between the string and rod (the lowermost in Figure 7), which the fluid must pass through. The pressure continues to grow until the contact opens. Subsequently, the pressure peak "jumps" to the next closed contact. Once again, the peak grows until the contact opens. This process of continuous opening observed in the smooth reference seal (Figure 5) is thus replaced by a stepwise opening phenomenon.

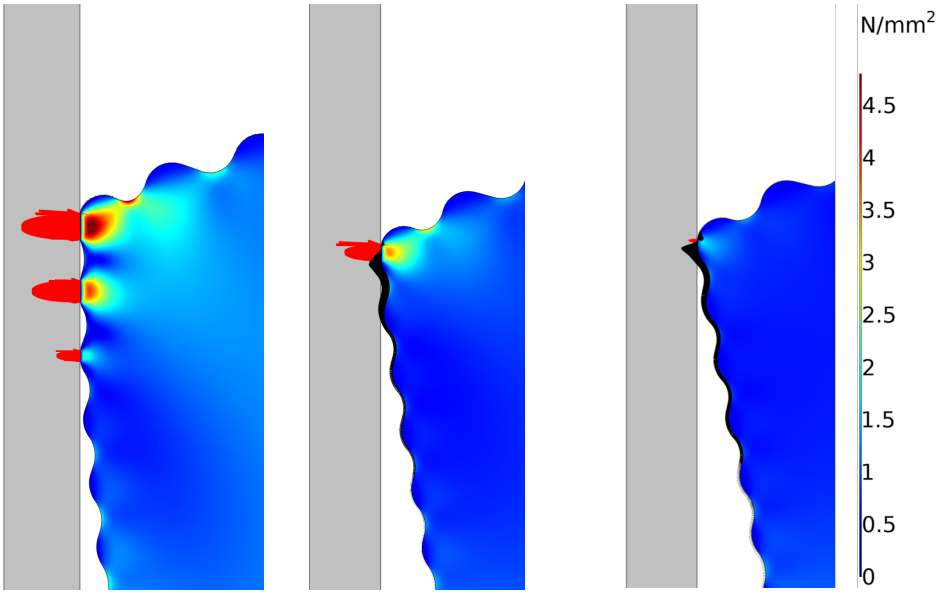

Figure 7: Contact pressure on the seal with FFF geometry. Red: Load from solid body contact between seal and rod. Black: Hydrodynamic load from the fluid.

A small region of solid body contact persists up to the maximum sliding velocity of $2\,m/s$, as illustrated in Figure 8. It becomes apparent that the transition of load from solid body contact to the fluid is no longer continuous but rather step-like. This corresponds to the locally discrete loss of contact for individual strings. This phenomenon occurs because the local converging rate at the seal gap differs between the smooth reference surface and the FFF surface generated by multiple strings.

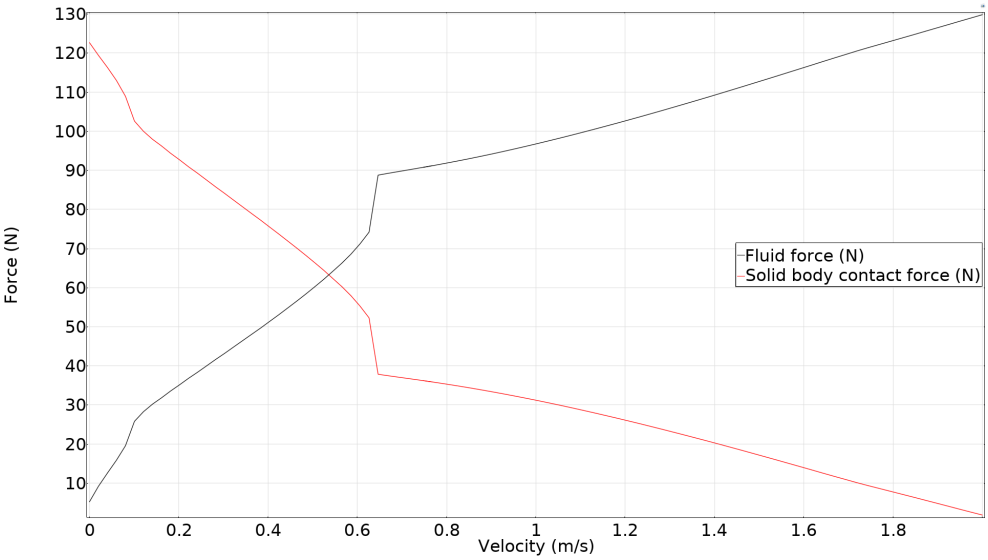

Figure 8: Velocity dependency of the load for the FFF geometry.

4.3 Consequences for fluid flow

In the fluid transport through the seal gap, drag flow predominantly occurs, which is carried with the moving rod through the seal gap against a pressure difference of $1.5\ bar$. To examine fluid transfer through the seal gap, the velocity field is integrated over the cross-section of the annular gap. Figure 9 illustrates the velocity-dependent mass flow. For velocities significantly lower than $1.86\ m/s$, the expected linear relationship between velocity and volumetric flow rate is observed. The linear behavior is nearly identical for both surface structures since the model assumes that the minimum distance between the rod and seal is identical: $2.0\ \mu m$. Smaller differences between both curves arise from the discrete loss of contact for individual strings and are not anticipated to be relevant in practical applications.

At higher sliding velocities, differences in the volumetric flow rate emerge: the smooth reference surface permits a higher volumetric flow rate compared to the FFF structure. The reason for this is that the smooth reference surface, with its continuously converging gap, loses solid body contact at significantly lower sliding velocities compared to the FFF structure. The dimples between individual strings reduce the gap's capability for continuous pressure buildup, as depicted in Figure 10. Consequently, solid body contact persists at sliding velocities higher than $1.86\ m/s$. Since at $2\ m/s$ the smallest seal gap is smaller for the FFF case ($2.0\ \mu m$) compared to the smooth reference case ($2.6\ \mu m$), the capability for fluid transport is higher in the smooth reference case.

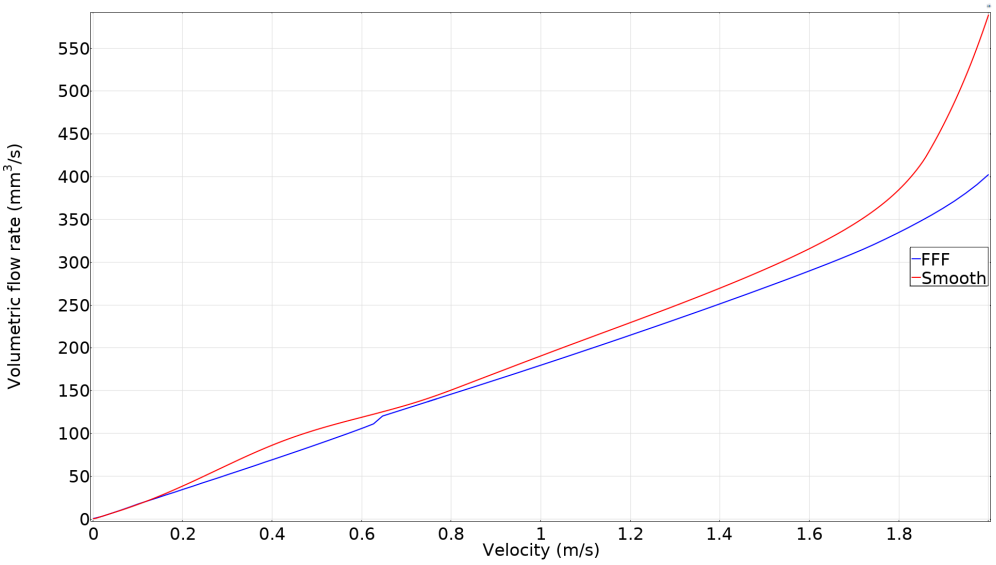

Figure 9: Maximum volumetric flow rate depending on rod velocity.

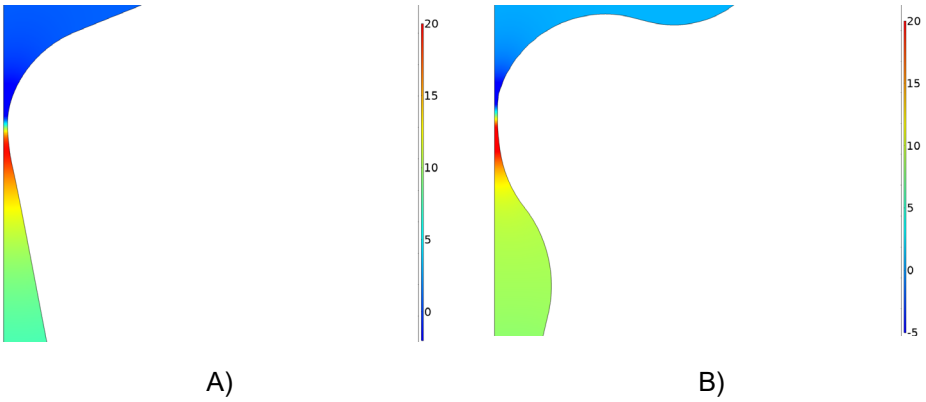

Figure 10: Comparison of fluid pressure distribution and seal gap height at $2\ m/s$. A) For smooth reference seal structure and. B) for FFF seal structure.

5 Summary and Conclusion

This numerical study employs FSI simulation to compare the fluid transport capability of dynamic rod seals during instroke back into the cylinder, against a background cylinder pressure of $1.5\ bar$. The primary transport mechanism is drag flow induced by translational motion. Two geometries are compared, differing in their local micro-structure on the seal lip: a conventional smooth reference and one inspired by the string structure of an FFF additive manufacturing process.

Key findings include:

- The FFF structure results in periodically fragmented contact with local pressure distributions similar to Hertz-type.
- Both structures exhibit very similar transport capabilities as long as they maintain solid body contact between the outermost seal tip and the rod.
- The continuously converging gap of the smooth reference surface enables the loss of solid body contact at lower velocities compared to the FFF structure. In the latter, the dimples between individual strings reduce the ability to establish a pressure peak, thereby preserving solid body contact to higher sliding velocities.
- Consequently, for higher rod velocities, the transport capability of the smooth reference seal is significantly higher compared to the FFF structure.

The model utilized in this study fully couples a fluid domain represented by the Navier-Stokes equation with a solid body domain. No free fluid surface for the ambient space was included. In practical applications, the volumetric flow during instroke is limited by the film thickness on the rod. Therefore, the computed volume flow in this study does not precisely represent the actual volumetric flow but rather provides the maximum possible transport rate that a dynamic rod seal allows.

These results suggest that seals with an FFF structure can be expected to exhibit similar transport capability compared to their smooth reference counterparts as long as they are not operated under conditions of full hydrodynamic lubrication, i.e., on the right side of the Stribeck curve.

6 Acknowledgements

This research has been partially funded by the Deutsche Forschungsgemeinschaft (DFG), project number 447009134. The authors would like to express their gratitude to the "Deutsches Institut für Kautschuktechnologie e.V." for their valuable discussions.

7 References

[1] Graf, M., Ebel, T., Lankenau, T. Ottink, K.: *Towards additively manufactured dynamic rod seals*, in: 21st International Sealing Conference Stuttgart 2022, Stuttgart, Germany, pp. 47-62, October 12-13, 2022

[2] Ebel, T., Lankenau, T., Sundermann, L., et al.: *Functional Testing of entirely additively manufactured two-component hydraulic rod seals made of TPU and NBR*, Discover Mechanical Engineering, Vol. 3, article number 4, 2024, https://doi.org/10.1007/s44245-024-00034-x

[3] Müller, H. K.; Nau, B. S.: www.fachwissen-dichtungstechnik.de *Kapitel 5 Hydraulikdichtungen*, accessed 27-02-2024

[4] Blok, H.*: Inverse problems in hydrodynamic lubrication and design directives for lubricated flexible surfaces*, Symp. Lub. and Wear, Houston, 1963

[5] Öngün, Y., André, M., Bartel, D, Deters, L.: *An axisymmetric hydrodynamicinterface element for finite-element computation of mixed lubrication in rubber seals*, Proceedings of the Institution of Mechanical Engineers, Part J: Journal of Engineering Tribology, 222, p. 471-481, 2008, https://doi.org/10.1243/13506501JET393

[6] Salant, R. F., Maser, N., Yang, B.: *Numerical Model of a Reciprocating Hydraulic Rod Seal*, Journal of Tribology 129-1, p. 91-97, 2007, https://doi.org/10.1115/1.2401222

[7] Lankenau, T., Graf, M., Ottink, K. Ebel, T.: *Simulation Strategy for Fluid-Structure Interaction of a Pre-tensioned Dynamic seal*, Proceedings in Applied Mathematics and Mechanics, Vol. 22, Issue 1, 2023, https://doi.org/10.1002/pamm.202200046

[8] Wennehorst, B., Poll, G.: *Soft micro-elastohydrodynamic lubrication and friction at rough conformal contacts*, Proceedings of the Institution of Mechanical Engineers, Part J, 231:3, pp. 302-315, https://doi.org/10.1177/1350650114558322

[9] v. Wahl*, H., Richter, T., Frei, S., Hagemeier, T.: Falling balls in viscous fluid with contact: Comparing numerical simulations with experimental data*, Physics of Fluids, 33, 03304, 2021, https://doi.org/10.1063/5.0037971

8 Authors

University of Applied Sciences Hochschule Emden/Leer

Constantiaplatz 4, 26723 Emden, Germany:

Matthias Graf, Prof. Dr.-Ing., ORCID 0000-0001-9999-7768,
matthias.graf@hs-emden-leer.de

Tobias Lankenau, M. Eng., ORCID 0000-0001-8105-0082,
tobias.lankenau@hs-emden-leer.de

Kathrin Ottink, Prof. Dr.-Ing., ORCID 0000-0002-5977-5316,
kathrin.ottink@hs-emden-leer.de

Thomas Ebel, Dr.-Ing., ORCID 0000-0003-2099-763X,
thomas.ebel@hs-emden-leer.de

https://doi.org/10.61319/IBIZNW2S